Article:
Yang, H., Chen, X., Lin, H. et al. (2 more authors) (2019) On-load demagnetization effect of high-coercive-force PMs in switched flux hybrid magnet memory machine. AIP Advances, 9 (12). 125152.

https://doi.org/10.1063/1.5130518

On-load demagnetization effect of high-coercive-force PMs in switched flux hybrid magnet memory machine

Cite as: AIP Advances **9**, 125152 (2019); https://doi.org/10.1063/1.5130518
Submitted: 27 October 2019 . Accepted: 24 November 2019 . Published Online: 30 December 2019

Hui Yang, Xiaomin Chen, Heyun Lin, Z. Q. Zhu, and Shukang Lyu

On-load demagnetization effect of high-coercive-force PMs in switched flux hybrid magnet memory machine

Cite as: AIP Advances 9, 125152 (2019); doi: 10.1063/1.5130518
Presented: 8 November 2019 • Submitted: 27 October 2019 •
Accepted: 24 November 2019 • Published Online: 30 December 2019

Hui Yang,[1,a)] Xiaomin Chen,[1] Heyun Lin,[1] Z. Q. Zhu,[2] and Shukang Lyu[1]

AFFILIATIONS

[1]School of Electrical Engineering, Southeast University, Sipailou 2, 210096 Nanjing, China
[2]Department of Electronic and Electrical Engineering, University of Sheffield, Mappin Street, Sheffield S1 3JD, UK

Note: This paper was presented at the 64th Annual Conference on Magnetism and Magnetic Materials.
[a)]huiyang@seu.edu.cn

ABSTRACT

In the previous researches of hybrid magnet memory motors (HMMMs), the demagnetization characteristics of low-coercive-force (LCF) magnets have been already investigated extensively. Nevertheless, the possible irreversible demagnetization of high-coercive-force (HCF) magnets remains unexplored hitherto. In this paper, the demagnetization behaviour of HCF magnets in switched flux hybrid magnet memory machines (SF-HMMMs) accounting for the high-level current pulse is revealed and investigated. A simplified magnetic circuit model is built to illustrate when and how the DC current pulse poses the risk of irreversible demagnetization to the HCF magnets. Furthermore, the influences of temperature, DC current amplitude and HCF magnet thickness on the irreversible demagnetization effect of HCF magnets in the investigated SF-HMMM are analyzed based on finite-element (FE) analyses. The theoretical and FE results are experimentally verified by the tests on an SF-HMMM prototype.

I. INTRODUCTION

Recently, memory machines (MMs)[1] are of growing research interests since the magnetization state (MS) of the low-coercive-force (LCF) magnets can be conveniently magnetized/demagnetized with a current pulse. In order to realize a convenient magnetization control, thereafter, switched flux hybrid magnet memory machines (SF-HMMMs)[2,3] equipped with both high-coercive-force (HCF) and LCF magnets are proposed to achieve high-efficiency operation within a wide speed range. Although the parallelity between permanent magnets (PMs) and armature fields in the proposed SF-HMMMs leads to advantageous demagnetization withstand capability, the potential partial irreversible demagnetization issue is a major concern. In addition, the previous literatures[4–9] about MMs mainly focus on the demagnetization of LCF magnets. Nevertheless, no insight has been provided into the irreversible demagnetization behaviour of HCF magnets hitherto, especially accounting for the influence of the high-level transient current pulse on HCF magnets. Thus, the purpose of this paper is to comprehensively investigate the demagnetization characteristics of HCF magnets in SF-HMMMs.

II. SF-HMMM MACHINE CONFIGURATION AND MAGNETIC CIRCUIT MODELING

The topology of the investigated SF-HMMM with 6-/13-pole configuration is shown in Fig. 1 (a).[10] The tangentially magnetized NdFeB PMs are inserted into the stator teeth and the radially magnetized LCF PMs between the outer stator ring and the inner stator segments. The MS and polarities of the LCF PMs can be changed by applying DC current pulses fed by the magnetizing coils wound around the LCF PMs. The corresponding flux distributions in the states of flux enhanced and flux weakened are shown in Figs. 1 (b) and (c), respectively.

Before the analysis of the demagnetization characteristics of HCF magnets, it is essential to determine how and when the HCF

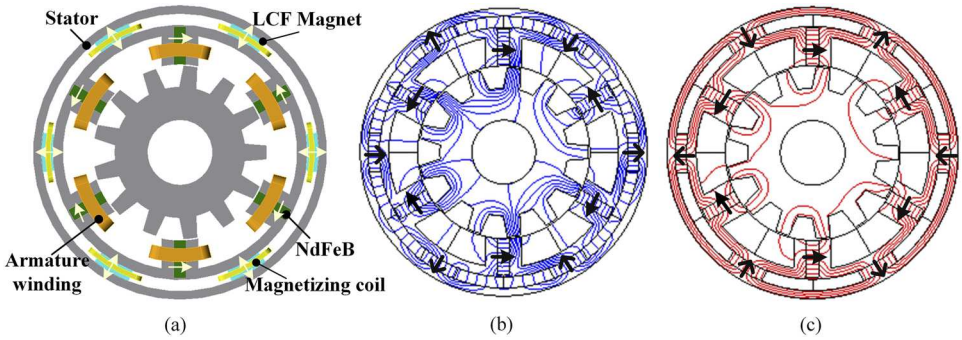

FIG. 1. (a) Topology of the investigated SF-HMMM, and open-circuit field distributions of the investigated SF-HMMM under (b) Flux enhanced, as well as (c) Flux weakened states.

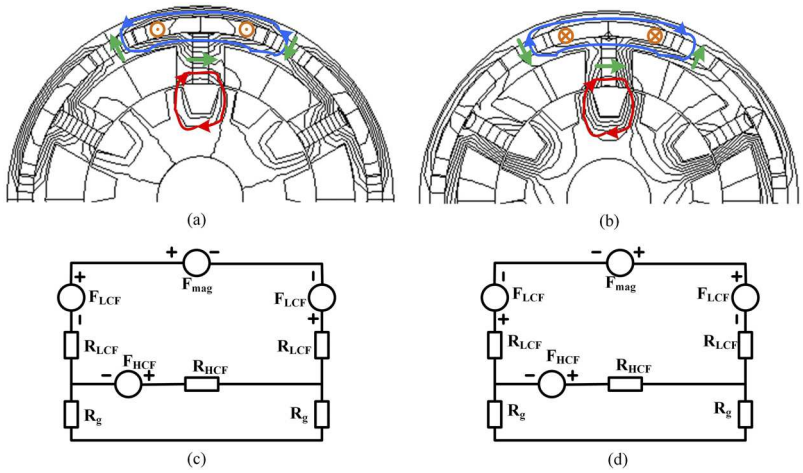

FIG. 2. Flux line distributions when LCF magnets are subject to (a) demagnetization and (b) remagnetization, and the corresponding simplified magnetic circuits when LCF magnets are subject to (c) demagnetization and (d) remagnetization.

magnets face the risk of irreversible demagnetization. With the assistance of finite element (FE) calculation, the flux lines corresponding to the transients when LCF magnets are subject to demagnetization and remagnetization by DC current pulse are shown in Figs. 2 (a) and (b), respectively. The major flux paths are highlighted with colored lines with arrows to indicate the circulating direction. Based on the field plot patterns, the simplified magnetic circuit is subsequently modeled to highlight the major flux paths in the machine, making it easier to visualize the relatively complex interactions between the magnetic elements. The corresponding simplified magnetic circuits ignoring the reluctance of core are shown in Figs. 2 (c) and (d), respectively. The circulating fluxes Φ_{demag} and Φ_{remag} at the HCF magnet branches when the LCF magnets are demagnetized and remagnetized by DC current pulse can be analytically formulated as:

$$\phi_{demag} = \frac{(4R_1R_g + 2R_2R_g)(F_{HCF} + F_{mag} - 2F_{LCF}) + 2R_1(2R_1 + R_2)F_{HCF}}{(2R_1 + R_2)(4R_1R_g + 2R_2R_g + 2R_1R_2)} \tag{1}$$

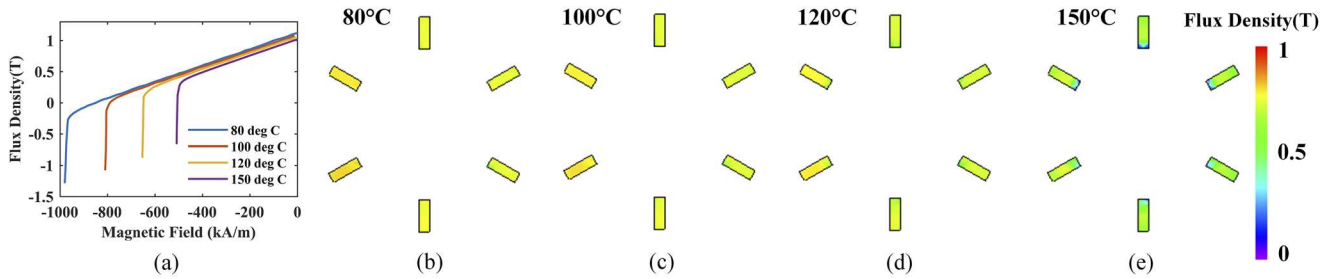

FIG. 3. (a) B-H curve of N35SH Magnetic flux density contour plot of the HCF magnets after the current pulse is withdrawn at (b) 80°C, (c) 100°C, (d) 120°C and (e) 150°C.

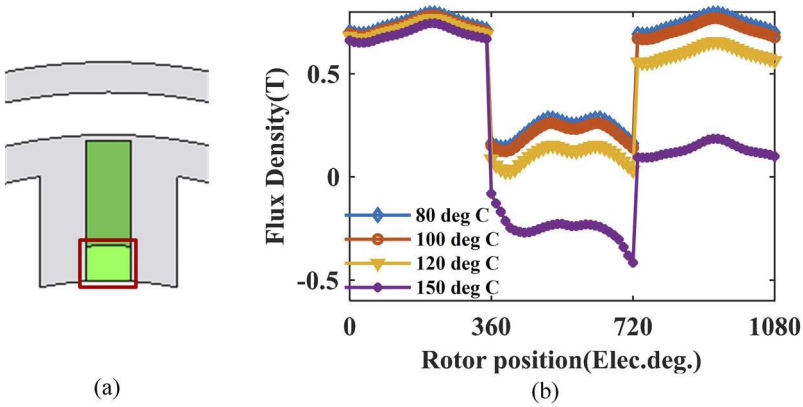

FIG. 4. (a) The 1/4 part of HCF magnets near the air-gap (b) Variation of average magnetic density.

$$\phi_{remag} = \frac{(4R_1R_g + 2R_2R_g)(F_{HCF} - F_{mag} + 2F_{LCF}) + 2R_1(2R_1 + R_2)F_{HCF}}{(2R_1 + R_2)(4R_1R_g + 2R_2R_g + 2R_1R_2)} \quad (2)$$

where F_{LCF} and F_{HCF} are the magnetomotive forces (MMFs) of LCF magnets and HCF magnets, respectively, R_{LCF} and R_{HCF} are the magnetic reluctances of LCF magnets and HCF magnets, respectively, F_{mag} is the MMF due to the current pulse to demagnetize/magnetize LCF magnets, and R_g is the air-gap magnetic reluctance.

In the case of LCF PM demagnetization, it can be analytically inferred from (1) that the HCF magnets fluxes rise with the increase of F_{mag}. This indicates that HCF magnets are unable to be demagnetized since the resultant MMF circulating the HCF PM branch shares the same direction with the magnetization direction of HCF magnets. On the other hand, in the case of LCF magnets remagnetization, as shown in (2), the HCF magnets fluxes drop with the increase of F_{mag}. The magnetic circuits demonstrate that only when the LCF magnets are remagnetized by DC current pulse, the HCF magnets will be prone to the demagnetization risk. Therefore, the analysis of the demagnetization characteristics of HCF magnets should be concentrated on the transient state when the LCF magnets are remagnetized.

III. DEMAGNETIZATION ASSESSMENT OF HCF MAGNETS

A. Influence of temperature

Firstly, the B-H curves of the HCF magnets (NdFeB PMs) are given in Fig. 3 (a) in advance, which provides a benchmark for the following analyses. It shows that as the temperature increases, the knee point of the PM moves from the third quadrant to the second one, and consequently the probability of irreversible demagnetization on the PM increases. In this case, a DC current of 40A is supplied considering the DC-voltage limitation. Meanwhile, the temperature is set within the range of 80 ~ 150 °C in order to confirm the safety margin. It is worth noting that the influence of the transient current pulse (usually lasts 50~100 ms) on the temperature can be neglected. Figs. 3(b)–(e) show the variation of working points in the HCF magnets after the current pulse is withdrawn at different temperatures, confirming the possibility of irreversible demagnetization due to high temperature. In particular, it can be easily found that the 1/4 part of HCF magnets near the air gap illustrated in Fig. 4 (a) are more vulnerable to demagnetization. Fig. 4 (b) shows the fluctuation of the average magnetic density of the 1/4 part of HCF magnets near the air-gap as a current pulse demagnetizing the HCF magnets is applied in the middle period. To evaluate the level of the localized demagnetization of HCF magnets, the demagnetization coefficient k_{demag} is defined as follows:

$$k_{demag} = \left(1 - \frac{B_{a2}}{B_{a1}}\right) \quad (3)$$

TABLE I. Demagnetization coefficients under various DC current amplitudes and temperatures.

	20A	40A	60A	80A
80°C	0.1%	0.3%	0.1%	0.1%
100°C	0.1%	2.1%	6.5%	13.9%
120°C	0.9%	16.2%	28.2%	41%
140°C	22.5%	70.4%	117.9%	139.4%

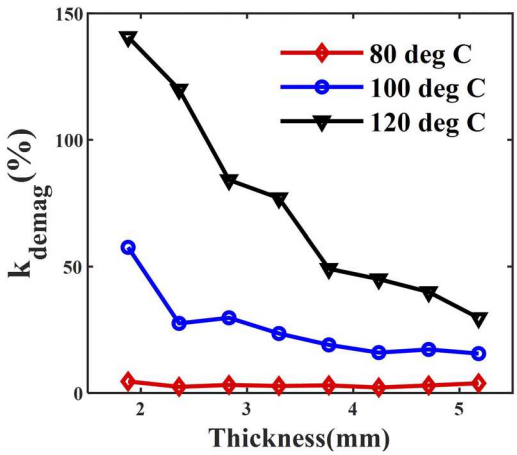

FIG. 5. Variation of the demagnetization coefficient with the thickness of HCF magnets.

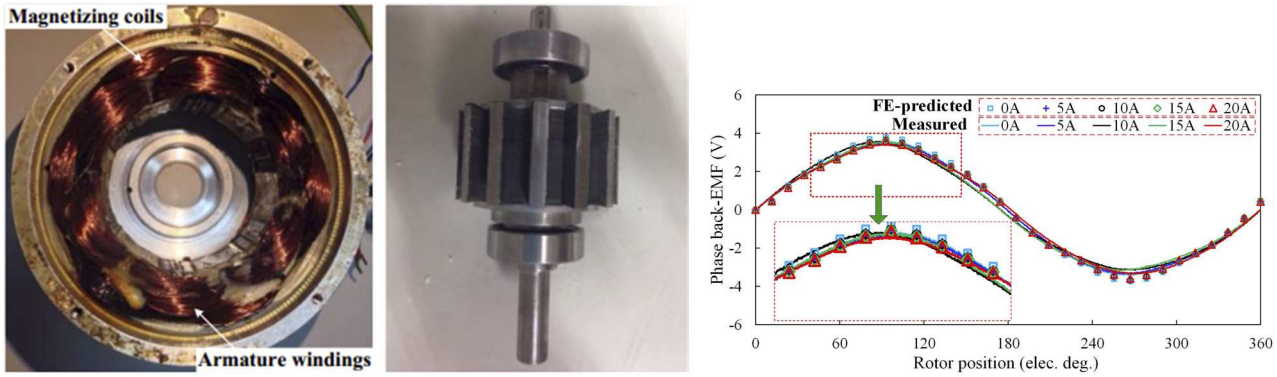

FIG. 6. The 6/13-pole SF-HMMM prototype and comparison of FE-predicted and measured open-circuit back-EMF (a) Stator assembly (b) Rotor assembly (c) Open-circuit back-EMF waveforms.

where B_{a1} is the average magnetic density of the 1/4 partial HCF magnets near the air-gap before applying the current pulse, while B_{a2} is the average magnetic density after the current pulse. Thus, the values of k_{demag} at 80°C, 100 °C, 120 °C and 150 °C are 2.8%, 4.5%, 18.5% and 81.1%, respectively. When the temperature of the machine rises from 120 °C to 150 °C, k_{demag} decreases rapidly, and the partial demagnetization of HCF magnets gets worse.

B. Influence of DC current pulse amplitude

The amplitude of DC current is another influencing factor for the demagnetization of HCF magnets. The resultant demagnetization coefficients k_{demag} under various DC current amplitudes at different temperatures are listed in Table I. "k_{demag} >100%" implies that HCF magnets are reversely remagnetized. From Table I, it shows that the demagnetization is more likely to occur with increasing the amplitude of DC current pulse. Nevertheless, the influence of the temperature turns out to be more pronounced. That is to say, the higher the temperature of the motor is, the stronger the impact of the DC current on the demagnetization of HCF magnets is.

C. Influence of HCF PM sizing

The influence of the HCF magnets thickness on its demagnetization is also explored. The demagnetization coefficient k_{demag} versus HCF magnet thickness curves subject to different temperatures are shown in Fig. 5. In general, the increase of HCF magnet thickness is beneficial to the on-load demagnetization withstand capability. Thus, the thickness of HCF magnet needs to be designed as sufficiently high to resist the high-temperature demagnetization.

IV. EXPERIMENT

An SF-HMMM prototype with 6-/13-pole configuration is manufactured and tested to verify the foregoing theoretical analyses. The stator/rotor assemblies are shown in Figs. 6 (a) and (b), respectively. The FE-predicted and measured open-circuit back-EMF waveforms are compared as shown in Fig. 6 (c). Due to the good thermal dissipation, the temperature of the stator is about 80°C in the rated-state, the HCF magnets can resist the impact of the high-level current pulse, making the SF-HMMM maintain high performance.

V. CONCLUSIONS

The unintentional demagnetization characteristics of HCF magnets in an SF-HMMM is investigated subject to a high-level transient current pulse. First, it can be found that the demagnetization of HCF magnets possibly occurs only in the LCF magnet remagnetization process. In addition, it shows that the on-load demagnetization withstand capability of HCF magnets can be improved when increasing HCF magnet thickness and lowering the current pulse level. Nevertheless, the temperature is a more predominant factor for the demagnetization behaviour of HCF magnets. If the temperature of the motor is designed as low enough, the effects of other factors on the demagnetization of HCF magnets turns out to be negligible. Thus, good thermal management is important for SF-HMMMs to maintain high performance especially accounting for the high-level current pulse. Finally, the experiments are carried out to confirm the theoretical analyses.

ACKNOWLEDGMENTS

This work was jointly supported in part by National Natural Science Foundations of China under Grant 51377036, in part by Natural Science Foundation of Jiangsu Province for Youth (BK20170674), in part by the Fundamental Research Funds for the Central Universities (2242017K41003), in part by "Hong Kong Scholar" Program (XJ2018014), and in part by Supported by the "Zhishan Youth Scholar" Program of Southeast University (2242019R40042).

REFERENCES

[1] V. Ostovic, IEEE Ind. Appl. Mag. **9**, 52 (2003).
[2] H. Yang, Z. Q. Zhu, H. Lin, P. Xu, H. Zhan, S. Fang, and Y. Huang, IEEE Trans. Energy Convers. **32**, 65 (2017).
[3] H. Yang, Z. Q. Zhu, H. Lin, D. Wu, H. Hua, S. Fang, and Y. Huang, IEEE Ind. Appl. **52**, 3901 (2016).

[4]H. Liu, H. Lin, S. Fang, and Z. Q. Zhu, IEEE Trans. Magn. **45**, 4736 (2009).
[5]J. H. Lee and J. P. Hong, IEEE Trans. Magn. **44**, 1550 (2008).
[6]X. Zhu, Z. Xiang, L. Quan, W. Wu, and Y. Du, IEEE Trans. Ind. Elec. **65**, 5353 (2018).
[7]H. Yang, H. Lin, Z. Q. Zhu, and S. Lyu, AIP Advances **8**, 056602 (2018).
[8]X. Zhu, J. Huang, L. Quan, Z. Xiang, and B. Shi, IEEE Trans. Ind. Elec. **66**, 2613 (2019).
[9]X. Zhu, D. Fan, L. Mo, Y. Chen, and L. Quan, IEEE Trans. Ind. Elec. **66**, 641 (2019).
[10]S. Lyu, H. Yang, H. Lin, Z. Q. Zhu, H. Zheng, and Z. Pan, IEEE Trans. Magn. **55**, 1 (2019).